European Journal of Taxonomy 1007: 1–23
https://doi.org/10.5852/ejt.2025.1007.2997

europeanjournaloftaxonomy.eu
ISSN 2118-9773
2025 · Chen H.-P. *et al.*

Received: 14 October 2024 • *Accepted: 8 April 2025* • *Published: 4 August 2025*

Topic editor: Tony Robillard • *Section editor: Gavin Broad* • *Desk editor: Pepe Fernández*

Research article

urn:lsid:zoobank.org:pub:CF496970-ABF2-4182-96B1-08187B7CDC0B

Montichneumon, a new genus of Ichneumoninae (Hymenoptera, Ichneumonidae) from the high mountains of Taiwan

Hsuan-Pu CHEN [1], Namiki KIKUCHI [2] & Shiuh-Feng SHIAO [3,*]

[1,3]Department of Entomology, National Taiwan University, No. 1, Sec. 4, Roosevelt Rd., Da'an Dist., Taipei 106, Taiwan.
[2]Toyohashi Museum of Natural History, 1-238 Oana, Oiwa, Toyohashi, Aichi 441-3147, Japan.
[2]Systematic Zoology Laboratory, Department of Biological Sciences, Graduate School of Science, Tokyo Metropolitan University, 1-1 Minamiosawa, Hachioji-shi, Tokyo, 192-0397, Japan.

[*]Corresponding author: sfshiao@ntu.edu.tw
[1]Email: pooh890510@gmail.com
[2]Email: namikikikuchi@gmail.com

Abstract. A new genus and species, *Montichneumon* Chen & Kikuchi gen. nov. and *Montichneumon immortalibestia* Chen & Kikuchi gen. et sp. nov., are described from the high mountains of Taiwan. This new genus is identified as belonging to the *Amblyteles* genus-group (previously known as subtribe Amblytelina, tribe Ichneumonini). The status of the new genus is confirmed based on morphological comparison and a multigene phylogeny using concatenated 28S and COI sequences. *Montichneumon* can be distinguished from other related genera by its enlarged second segment of maxillary palps, smooth and sparsely punctate postpetiole, weakly convex scutellum without lateral carina, and narrow, elongate gastrocoelus. The new genus is compared with morphologically similar genera *Achaius* Cameron, 1903, *Achaiusoides* Tereshkin, 2011, *Diphyus* Kriechbaumer, 1890, *Hepiopelmus* Wesmeal, 1845, *Limerodops* Heinrich, 1949, *Serratichneumon* Riedel & Sheng, 2023, and *Tricholabus* Thomson, 1894. A diagnostic key to these morphologically similar genera of the *Amblyteles* genus-group is provided, and the generic position of this new genus is also discussed.

Keywords. Darwin wasp, generic placement, molecular phylogeny, high-elevation, taxonomy.

Chen H.-P., Kikuchi N. & Shiao S.-F. 2025. *Montichneumon*, a new genus of Ichneumoninae (Hymenoptera, Ichneumonidae) from the high mountains of Taiwan. *European Journal of Taxonomy* 1007: 1–23. https://doi.org/10.5852/ejt.2025.1007.2997

Introduction

Ichneumoninae Latreille, 1802 represents the most diverse subfamily of Darwin wasps, comprising at least 425 described genera and over 4300 species with cosmopolitan distribution (Yu *et al.* 2016; Claridge *et al.* 2023; Sheng *et al.* 2023). Due to its high species diversity and challenges in identification, this subfamily has limited comprehensive taxonomic studies (although better-served than other very

diverse ichneumonid subfamilies) and higher-level classification work. This gap hinders the training of future taxonomists and engagement of citizen scientists in studying this group (Santos *et al.* 2021; Dal Pos *et al.* 2023a).

The classification system of Ichneumoninae was primarily established through the works of Heinrich (e.g., Heinrich 1967a, 1967b, 1974a, 1977), who subdivided the subfamily into 18 tribes (Tereshkin 2009; Yu *et al.* 2016). However, the ultraconserved elements (UCEs) phylogenomic study of Santos *et al.* (2021) revealed that the previous tribal classification system was based on characters which have undergone convergent evolution and did not accurately reflect the evolutionary history of this subfamily. Consequently, the tribal classification has been simplified to seven tribes, incorporating 11 previous tribes within the mega-tribe Ichneumonini Latreille, 1802 and synonymizing the previous subtribes of Ichneumonini due to their non-monophyly (Santos *et al.* 2021).

The ichneumonine fauna of the Oriental region remains less studied compared to that of the Holarctic region, evidenced by the scarcity of publications and the absence of comprehensive, up-to-date keys and revisions (e.g., Townes *et al.* 1961; Heinrich 1965a, 1965b, 1966, 1967c, 1968a, 1968b, 1969, 1970, 1974a, 1974b, 1975, 1980; Gupta 1988; Riedel 2019, 2023; Sheng *et al.* 2023; Chen *et al.* 2024). Given the high abundance and species diversity of Ichneumoninae in Neotropical habitats (Gauld 1991; Veijalainen *et al.* 2013; Claridge *et al.* 2023), the species diversity of Ichneumoninae in the Tropical and Subtropical Oriental regions is probably under-described, although it should be noted that even fewer species have been described from the Neotropics, where there have been some demonstrations of actual species richness, lacking in the Oriental region.

During faunistic investigations in the high-elevation mountains of Taiwan, a remarkable species was discovered and identified as a member of the subtribe "Amblytelina" Viereck, 1918 sensu Heinrich (1967a) (currently synonymized within Ichneumonini) using the key of Tereshkin (2009). After a morphological comparison with all known genera previously classified within "Amblytelina", combined with a multigene molecular phylogenetic analysis, this species was confirmed to be new to science and belongs to a new genus. This new genus and species are described herein. A diagnostic key to morphologically similar genera is provided, and the generic placement of this new genus is discussed.

Material and methods

Morphological examination and description

The general morphological terms used in this study are as per Broad *et al.* (2018), except those of metasomal sternites as per Kikuchi & Konishi (2021) and male genitalia as per Dal Pos *et al.* (2023b). Measurements were performed as per Kikuchi & Konishi (2021), and the abbreviations used in this study as per Chen *et al.* (2024). The metasomal sternites and male genitalia were macerated using Proteinase K and dissected for detailed observation. The cuticular macrosculpture is described as per Eady (1968). The measurements in parentheses represent the measurements of the holotype.

Specimens were examined and measured using a microscope Leica S8 APO (Leica Microsystems, Wetzlar, Germany) with an electronic micrometer (TEKFAR Inc., Taichung, Taiwan). Photographs were taken using a Leica DMC 5400 camera integrated into a Leica Z16 APO microscope equipped with the auto-stacking system Leica LAS ver. 4.13 (all from Leica Microsystems). Line drawings were made using Procreate (Savage Interactive, Hobart, Australia). All figures were edited and arranged into figure plates using Adobe Illustrator CC and Photoshop CC (Adobe Systems, San Jose, CA, USA). The specimens and their photos examined in this study were deposited in the National Museum of Natural Science, Taichung, Taiwan (NMNS), Department of Entomology, National Chung Hsing University, Taichung, Taiwan (NCHU). Additional specimens and photos for comparison were deposited at the Taiwan Forestry Research Institute, Taipei, Taiwan (TFRI) or accessed online

from the following websites: BioImages (https://www.bioimages.org.uk/), WaspWeb: Hymenoptera of the World (https://www.waspweb.org/), Checklist of Japanese Ichneumonidae (Hymenoptera) (http://web.agr.ehime-u.ac.jp/~entomology/mokuroku/), and Zoologische Staatssammlung München, Ichneumoninae of G.H. Heinrich (https://zsm.snsb.de/sammlung/ichneumoninae-of-g-h-heinrich/?lang=en).

Molecular data collection and analysis

Genomic DNA was extracted from one right mid leg, male genitalia, or whole metasoma using DNeasy Blood and Tissue Kit (Qiagen, Düsseldorf, Germany). DNA sequences of two genetic markers, the mitochondrial cytochrome c oxidase I (COI) and D2–D3 regions of nuclear 28S ribosomal RNA gene (28S), were used for phylogenetic reconstruction. Target sequences were amplified by polymerase chain reaction (PCR), and the primer pairs and conditions used in this study are summarized in Table 1. The reaction volume was 15 μL : 4.3 μL of sterile distilled water, 0.6 μL of each forward and reverse primer (10 μM), 7.5 μL of GoTaq Green Master Mix (Promega, Madison, WI, USA), and 2.0 μL of DNA template. PCR products were purified and sequenced at Tri-I Biotech (Taipei, Taiwan). The software and settings used for sequence editing and alignment are as per Chen *et al.* (2024). All newly obtained sequences were uploaded on GenBank.

Taxon sampling

A dataset of Ichneumoniformes (the informal group of subfamilies to which Ichneumoninae belong), generated by editing the dataset of Chen *et al.* (2024), was employed to infer the generic placement of the target specimens by molecular phylogenetic reconstruction. This dataset comprised sequences for two genetic markers and included a total of 106 operational taxonomic units (OTUs), with 69 Ichneumoninae OTUs designated as the ingroup. The remaining OTUs served as outgroups and consisted of 24 Cryptinae Kirby, 1837, 11 Phygadeuontinae Förster, 1869, one Microleptinae Townes, 1958 (*Microleptes splendidulus* Gravenhorst, 1829), and one Agriotypinae Haliday, 1838 (*Agriotypus armatus* Curtis, 1832). The sequences excluding the newly collected specimens were obtained from the online database GenBank (Nation Center for Biotechnology Information) and BOLD systems (Ratnasingham & Hebert 2007; available at: http://v4.boldsystems.org/). Details regarding the included OTUs and sequences are provided in Supp. file 1.

Molecular phylogeny

The multigene phylogeny was reconstructed using the concatenated 28S plus COI dataset partitioned by gene for the 28S sequences, and for the protein-coding COI sequences, by codon position (first plus second versus third). ModelFinder (Kalyaanamoorthy *et al.* 2017) was used to search for the best partitioning scheme and substitutional models under the Bayesian Information Criteria.

The maximum likelihood (ML) method was used for phylogenetic reconstruction by using IQ-TREE ver. 1.6.12 (Nguyen *et al.* 2015) through the web server W-IQ-TREE (Trifinopoulos *et al.* 2016) (available at http://iqtree.cibiv.univie.ac.at/). Ultrafast bootstrap approximation (UFBoot) method (Minh *et al.* 2013) and the SH-like approximate likelihood ratio test (SH-aLRT) (Guindon *et al.* 2010) were employed to evaluate nodal support. Both methods were under the default setting of IQ-TREE ver. 1.6.12. Nodes with an SH-aLRT value of ≥80% and a UFBoot value of ≥95% were considered to be strongly supported. The tribal classification of Santos *et al.* (2021) was mapped on the reconstructed ML tree (Fig. 1).

Since the subtribe "Amblytelina" is no longer recognized, we use '*Amblyteles* genus-group' here which corresponds to the clade formed by *Achaius* Cameron, 1903, *Amblyteles* Wesmael, 1845, *Ctenichneumon* Thomson, 1894, *Diphyus* Kriechbaumer, 1890, *Eutanyacra* Cameron, 1903, *Ectopimorpha* Viereck, 1912, *Netanyacra* Heinrich, 1968, *Neodiphyus* Heinrich, 1977, *Oreohoplis* Townes, 1966, *Setanta* Cameron, 1901, and *Thymebatis* Brèthes, 1909 in Santos *et al.* (2021). Additional genera previously classified

Table 1. PCR primers and conditions used in this study. Regarding PCR conditions, 35 cycles were run for *COI*, whereas 30 cycles were run for *28S*. Abbreviation: PCR= polymerase chain reaction.

		PCR primers	
Markers	**Primers**	**Sequences (5′–3′)**	**References**
COI	Fol_Ich_F	TTTCAACAAATCATAAAGATATCGG	Chen *et al*. (2023)
	Fol_Ich_R	TAAACTTCAGGATGACCAAAAAATCA	
	LCO1490	GGTCAACAAATCATAAAGATATTGG	Folmer *et al*. (1994)
	HCO2198	TAAACTTCAGGGTGACCAAAAAATCA	
	Primer Mix F	LCO1490 : Fol_Ich_F = 1:1	This study
	Primer Mix R	HCO2198 : Fol_Ich_R = 1:1	
28S	(F)	GCGAACAAGTACCGTGAGGG	Laurenne *et al*. (2006)
	(R)	TAGTTCACCATCTTTCGGGTC	

	PCR conditions				
Markers	**Primary denaturation**	**Denaturation**	**Annealing**	**Extension**	**Additional extension**
COI	95°C, 4 min	95°C, 30 sec	47°C, 1 min	72°C, 45 sec	72°C, 10 min
28S	95°C, 4 min	96°C, 15 sec	50°C, 30 sec	72°C, 30 sec	75°C, 7 min

within "Amblytelina" but not included in Santos *et al.* (2021) – such as *Achaiusoides* Tereshkin, 2011, *Bureschias* Heinrich, 1936, *Fileanta* Cameron, 1901, *Hepiopelmus* Wesmeal, 1845, *Limerodes* Wesmeal, 1845, *Limerodops* Heinrich, 1949, *Obtusodonta* Heinrich, 1962, *Serratichneumon* Riedel & Sheng, 2023, *Spilichneumon* Thomson, 1894, *Triptognathus* Berthoumieu, 1904, and *Tricholabus* Thomson 1894 – are also presumably members of this genus-group and included for comparison.

Results

Molecular datasets

The concatenated 28S+COI dataset is composed of a total of 206 sequences, including 100 COI and 107 28S sequences. Among them, two sequences, COI and 28S of the holotype of the new genus and species, were newly generated. Five of the COI sequences were obtained from the BOLD system, and the remaining sequences were obtained from GenBank.

No pseudogenes (identifiable by the occurrence of stop codons in translated amino acid sequences) were identified from the COI alignment. The total length of the concatenated 28S+COI dataset is 1401 bp. The average length of the alignment is 1203 bp, with 43.7% of GC content, 756 variable sites, and 537 parsimony informative sites. The dataset used in this study is provided in Supp. file 2.

Molecular phylogeny

Figure 1 shows the ML phylogenetic tree of Ichneumoniformes reconstructed using the concatenated 28S+COI dataset. The result indicates that subfamily Ichneumoninae excluding Alomyini Förster, 1869 (*Alomya debellator* (Fabricius, 1775)) and *Phaeogenes* sensu lato sp. is a supported clade (SH-aLRT/UFBoot = 99.2/91). However, the tribe Ichneumonini is resolved as a polyphyletic group, with members of Platylabini, Phaeogenini, and Notosemini nested within. The members of the *Amblyteles* genus-group,

Fig. 1. Maximum-likelihood phylogenetic tree of Ichneumoninae Latreille, 1802 based on the concatenated 28S+COI dataset (1401 bp, 28S: 753 bp; COI: 648 bp; GTR+F+I+G4 (1–753, 754-1401\3, and 755-1401\3 bp); K3Pu+F+I+G4 (756-1401\3 bp)). The red color indicates the newly described taxa. The branch lengths are proportional to infer nucleotide substitutions per site except for the root *Agriotypus armatus* Curtis, 1832 branch. Circles on the nodes represent different degrees of 'SH-aLRT / UFBoot' values. Nodal supports with both SH-aLRT < 80% and UFBoot < 95% are not shown.

excluding *Setanta apicalis* (Uchida, 1926), *Ctenichneumon funereus* (Geoffroy, 1785), *Hepiopelmus melanogaster* (Gmelin, 1790), *Tricholabus strigatorius coreanus* (Uchida, 1926), and *Obtusodonta equitatoria* (Panzer, 1786), form a strongly supported clade (H-aLRT/UFBoot = 95.7/99). The newly collected species is nested within the *Amblyteles* genus-group and is sister to *Diphyus palliatorius* (Gravenhorst, 1829). However, the low support value suggests that its sister relationship remains uncertain. Given the morphological incongruences (see Table 2 and Diagnosis of *Montichneumon* Chen & Kikuchi gen. nov. below) between all known genera of the *Amblyteles* genus-group and the phylogenetic position of this species, which cannot be placed within any known genus, we believe that it is justifiable to describe the newly collected specimens as a new genus and new species, *Montichneumon immortalibestia* Chen & Kikuchi gen. et sp. nov.

Taxonomy

Class Insecta Linnaeus, 1758
Order Hymenoptera Linnaeus, 1758
Superfamily Ichneumonoidea Latreille, 1802
Subfamily Ichneumoninae Latreille, 1802
Family Ichneumonidae Latreille, 1802
Tribe Ichneumonini Latreille, 1802

Genus ***Montichneumon*** Chen & Kikuchi gen. nov.
urn:lsid:zoobank.org:act:C6E9DABA-07A7-4AE1-B593-CE264E2679F6
Figs 2–5

Type species

Montichneumon immortalibestia Chen & Kikuchi gen. et sp. nov., designated herein.

Diagnosis

This genus is identified as belonging to the *Amblyteles* genus-group (previous Amblytelina subtribe) based on the key of Tereshkin (2009) and can be separated from other Ichneumoninae tribes based on the following characters: face and clypeus divided by a groove (Fig. 3B); clypeus flat (Fig. 3B, D); propodeum with horizontal and declivous surfaces, the apex of the area dentipara distant from the base of the hind coxa (Figs 2A, 3A); propodeal spiracle linear (Fig. 3A); areolet pentagonal (Fig. 4A); female metasomal apex amblypygous (Fig. 2); thyridium indistinct (Figs 3G, 5D); male abdominal sternum 9 usually medially convex on the apical margin (Fig. 5E).

Montichneumon gen. nov. can be diagnosed from other genera of the *Amblyteles* genus-group in having the following combination of characters: flagellum lacking white annulus or semi-annulus (Fig. 2); malar space long in anterior view (Fig. 3B); mandible long and bidentate, evenly narrowed to apex with upper tooth longer than lower tooth (Fig. 4B); second segment of maxillary palps enlarged (Fig. 3D); scutellum weakly convex without lateral carina (Fig. 3H); propodeum at apex of area dentipara with small teeth, lacking strong teeth or apophysis (Fig. 3A); area basalis of propodeum lacking medial tubercle (Figs 3F, 5C); anterior transverse carina of propodeum present medially and absent laterally (Figs 3F, 5C); postpetiole of T1 flat and smooth with sparse punctures, lacking striae or rugae (Figs 3A, G, 5D); gastrocoelus long and narrow, shallowly impressed, thyridium indistinct (Figs 3G, 5D); T7 normal, not bending downwards laterally (Fig. 2B); metasomal sternites weakly sclerotized, with S2 and S3 unsclerotized with fold medially (Fig. 4D); male abdominal sternum 9 lacking medial process (Fig. 5E).

This genus is morphologically similar or closely related phylogenetically (Fig. 1) to the following genera: *Achaius*, *Achaiusoides*, *Amblyteles*, *Diphyus*, *Eutanyacra*, *Hepiopelmus*, *Limerodops*, *Serratichneumon*, *Spilichneumon*, and *Tricholabus*. *Montichneumon* gen. nov. is morphologically most similar to *Hepiopelmus* in having a smooth postpetiole and narrowed gastrocoeli but differs in the weakly convex scutellum and completely sclerotized female S4 (scutellum highly elevated and female S4 unsclerotized in *Hepiopelmus*); *Limedrodops* in having narrowed gastrocoeli and a similar metasoma shape but differs in the weakly convex scutellum and normal female T4–7 (scutellum highly elevated and lateral sides of female T4–T7 strongly bending downward ventrally in *Limedrodops*); *Achaiusoides* in having smooth and sparsely punctate postpetiole and enlarged second segment of maxillary palps but differs in the long area superomedia with lateral part of anterior transverse carina absent (area superomedia wide with lateral part of anterior transverse carina present in *Achaiusoides*); it is also similar to some Oriental species of *Diphyus* (e.g., *D. charlottae* (Heinrich, 1965), *D. malaisei* (Heinrich, 1965), *D. victoriae* (Heinrich, 1965), and *D. uliae* Sebalt, 2013) in having a yellow and black color pattern, weakly convex scutellum or narrowed gastrocoeli but differs in the smooth and sparsely punctate postpetiole and narrowed T1 (postpetiole striate and T1 wider in *Diphyus*).

The differential diagnosis between *Montichneumon* gen. nov. and its morphologically similar genera (genera mentioned above except *Amblyteles*, *Eutanyacra*, and *Spilichneumon*) is summarized in Table 2.

Etymology

The generic name '*Montichneumon*' is derived from the Latin dative singular noun '*monti*-' ('mountain') plus '*ichneumon*', reflecting that this new genus was collected from the high-elevation mountain of its type locality in Taiwan. The gender is masculine.

Description

Head (Fig. 3B–D). Mandible long and bidentate, evenly narrowed to apex with upper tooth longer than lower tooth; malar space longer than basal mandibular width; clypeus separated from face, flat and truncated in ventral margin; occipital carina strong and complete, meeting hypostomal carina above mandibular base; female flagellum bristle-shaped, slightly flattened medially and tapered apically; male flagellum with tyloids present on segments 9–19; flagellum lacking white annulus or semi-annulus.

Mesosoma (Fig. 3A, E–F). Epomia present; notaulus indistinct; scutellum weakly convex without lateral carina, not strongly elevated above postscutellum; sternaulus indistinct; posterior transverse carina of mesosternum only present laterally; juxtacoxal carina present; propodeal carinae indistinct with anterior transverse carina only present medially, and longitudinal carinae weakly developed to posterior apex; area basalis without medial tubercle.

Legs (Fig. 2). Legs slender; female hind coxa without scopa; tarsal claws simple, without pecten.

Wings (Fig. 4A). Fore wing with areolet pentagonal. Hind wing nervellus inclivous and intercepted below.

Metasoma (Figs 3F–G, 4C–D, 5D–G). Metasoma slender, parallel-sided and weakly tapering posteriorly; T1 flat in lateral view and smooth with sparse punctures; T2 polished, evenly (or sparsely) and minutely punctate; gastrocoelus indistinct, long and narrow, shallowly impressed; thyridium indistinct, transverse and narrower than interval between thyridia; female metasomal apex amblypygous; ovipositor not significantly projecting beyond metasomal apex; male abdominal sternum 9 convex on apical margin, without medial process; gonostyle simple.

Table 2 (continued on next page). Comparison of the diagnostic characters between *Montichneumon* gen. nov. and its morphologically similar genera. Abbreviation: OD = diameter of lateral ocelli.

	Montichneumon gen. nov.	***Achaius*** Cameron, 1903	***Achaiusoides*** Tereshkin, 2011	***Diphyus*** Kriechbaumer, 1890	***Hepiopelmus*** Wesmeal, 1845	***Limerodops*** Heinrich, 1949	***Serratichneumon*** Riedel & Shen, 2023	***Tricholabus*** Thomson, 1894
Distribution	Oriental	Palearctic, Oriental	Palearctic	Palearctic, Nearctic, Oriental, Neotropical, Afrotropical, Oceanic	Palearctic, Oriental	Palearctic, Nearctic	Oriental	Palearctic, Nearctic, Oriental, Neotropical
Female flagellum	Bristle-shaped, thin, not widened medially	Bristle-shaped, thin, not widened medially	Bristle-shaped, moderately thick, slightly widened medially	Bristle-shaped, thin to moderately thick, slightly widened medially	Bristle-shaped, thin, slightly widened medially	Bristle-shaped, thin, slightly widened medially	Bristle-shaped, thin, slightly widened medially	Bristle-shaped, thin, slightly widened medially
Male flagellum	Normal	Normal	Normal	Normal	Normal	Normal	Serrated	Normal
White annuli	Absent	Present	Present	Present	Absent	Present	Present	Present
Temples	Longer than OD	Less than OD	Equal to OD	Longer than OD	Equal to OD	Longer than OD	Equal to OD	Equal to OD
Occipital and hypostomal carina	Meeting above mandible base	Meeting above mandible base	Meeting above mandible base	Meeting above mandible base	Meeting above mandible base	Meeting above mandible base	Meeting above mandible base	Meeting at Mandible base
Malar space	Longer than mandible base	Equal to mandible base	Shorter than mandible base	Shorter than mandible base	Equal to mandible base	Shorter than mandible base	Equal to mandible base	Equal to mandible base
Mandibles	Bidentate, long, evenly narrowed	Bidentate, narrow, parallel-sided	Bidentate, short, evenly narrowed	Bidentate, long, evenly narrowed	Bidentate, long, evenly narrowed	Bidentate, long, evenly narrowed	Bidentate, short, evenly narrowed	Bidentate, short, evenly narrowed
Maxillary palps	Enlarged in 2nd segment	Not enlarged in 2nd segment	Enlarged in 2nd segment	Not enlarged in 2nd segment	Not enlarged in 2nd segment	Not enlarged in 2nd segment	Not enlarged in 2nd segment	Not enlarged in 2nd segment
Scutellum	Flat, without lateral carina	Highly elevated, without lateral carina	Highly elevated, without lateral carina	Highly elevated, without lateral carina	Highly elevated, without lateral carina	Elevated, without lateral carina	Elevated, without lateral carina	Highly elevated, without lateral carina
Area basalis	Without medial tubercle	Without medial tubercle	Without medial tubercle	Without medial tubercle	With medial tubercle	Without medial tubercle	With medial tubercle	Without medial tubercle
Area superomedia	Present, elongated	Present, elongated	Present, transverse	Present, square or rectangular	Present, square or rectangular	Present, square or rectangular	Absent or incomplete	Present, elongated
Apex of area dentipara	Small teeth	Small teeths	Broad teeth	Small teeth	Small teeth	Small teeth	Without any projections	Small teeth
T1 postpetiole	Flat and narrow, smooth and sparsely punctate	Elevated and broad, smooth and sparsely punctate	Elevated and narrow, smooth and sparsely punctate	Elevated and broad, striate	Elevated and broad, sparsely punctate with medial impression	Elevated and broad, striate	Elevated and broad, coarsely punctate and carinate	Elevated and broad, sparsely punctate

Table 2 (continued). Comparison of the diagnostic characters between *Montichneumon* gen. nov. and its morphologically similar genera. Abbreviation: OD = diameter of lateral ocelli.

	Montichneumon gen. nov.	***Achaius*** Cameron, 1903	***Achaiusoides*** Tereshkin, 2011	***Diphyus*** Kriechbaumer, 1890	***Hepiopelmus*** Wesmeal, 1845	***Limerodops*** Heinrich, 1949	***Serratichneumon*** Riedel & Shen, 2023	***Tricholabus*** Thomson, 1894
Gastrocoelus	Long and narrow, shallowly impressed	Small and shallowly impressed	Long and shallowly impressed	Small or long and narrow, and shallowly impressed	Small and deeply impressed	Long and narrow, deeply impressed	Short and wide, deeply	Short and wide, deeply
Thyridium	Indistinct, narrower than interval distance	Indistinct, narrower than interval distance	Distinct, equal to interval distance	Almost absent to distinct, narrower than interval distance	Distinct, narrower than interval distance	Almost absent or indistinct	Distinct, wider than interval distance	Distinct, equal to interval distance
T2 sculptures	Sparsely and minutely punctate	Minutely punctate with longitudinal striae	Densely and minutely punctate	Densely punctate	Densely and minutely punctate	Longitudinal striate	Densely and coarsely punctate	Densely punctate
T2–T3 shape	Distinctly longer than wide	Equal to or slightly longer than wide	Equal to or slightly longer than wide	Equal to or slightly longer than wide	Equal to or slightly longer than wide	Distinctly longer than wide	Equal to or slightly longer than wide	Equal to or slightly longer than wide
T7 shape	Normal	Normal	Normal	Normal	Normal	Strongly bent downward laterally	Normal	Normal
Female S6	Truncate in posterior margin	Truncate in posterior margin	Truncate in posterior margin	Truncate in posterior margin	Truncate in posterior margin	Pointed in posterior margin	Rounded in posterior margin	Pointed in posterior margin
Female metasomal sternites	S2–S3 unsclerotized with longitudinal fold	S2–S3 unsclerotized with longitudinal fold	S2–S3 unsclerotized with longitudinal fold	Only S2, or S2–S3 with longitudinal fold	S2 completely or largely unsclerotized, S3–S4 unsclerotized with longitudinal fold	S2–S4 completely sclerotized, or unsclerotized with longitudinal fold	S2–S4 unsclerotized with longitudinal fold	S2–S4 unsclerotized with longitudinal fold
Male abdominal sternum 9	Triangularly convex in apical margin	Triangularly convex in apical margin	Unknown	Triangularly convex in apical margin	Triangularly convex in apical margin	Triangularly convex in apical margin	rounded in apical margin	Convex in apical margin with swelling

Distribution

Taiwan.

Bionomics

See the Bionomics section of *M. immortalibestia* gen. et sp. nov. below.

Remarks

Sexual dimorphism in this genus is limited to body coloration (see Description of *M. immortalibestia* gen. et sp. nov. below).

Key to Palearctic and Oriental genera of the *Amblyteles* genus-group related to *Montichneumon* Chen & Kikuchi gen. nov. (modified from Tereshkin (2011) and Sheng et al. (2023))

1. Propodeum with strong, upcurved apophysis at apex of area dentipara ..... ***Amblyteles*** Wesmeal, 1845
– Propodeum toothless or with small or broad tooth at apex of area dentipara 2

2. Postpetiolus distinctly striate or longitudinally rugose 3
– Postpetiolus not distinctly striated, smooth, sparsely punctate, or weakly rugose 7

3. Gastrocoeli distinct and deeply impressed, with interspace strongly arcuate; thyridia absent; anterior sternites of metasoma completely or strongly sclerotized; abdominal sternum 9 of male (hypopygium) without median process at apex ..... ***Ctenichneumon*** Thomson, 1894
– Gastrocoeli variable from shallowly to deeply impressed, with interspace not arcuate; thyridia present, at least vestigial; anterior sternites of metasoma variable; abdominal sternum 9 of male with median process at apex 4

4. Mandibles of females normal or enlarged medially, with teeth blunt, flattened, or shortened; abdominal sternum 9 (hypopygium) of male with median process at apex long 5
– Mandibles of females normal, gradually narrowed apically with upper tooth longer than lower tooth; abdominal sternum 9 with median process at apex normal 6

5. S6 (hypopygium) of female with bunch of hard setae apically; propodeum in lateral profile with dorsal surface shorter than posterior surface; area superomedia wider than long or square ..... ***Eutanyacra*** Cameron, 1903
– S6 of female without bunch of hard setae apically; propodeum in lateral profile with dorsal surface longer than posterior surface; area superomedia always longer than wide ..... ***Spilichneumon*** Thomson, 1894

6. Metasoma strongly elongate and narrowed posteriorly in female, but parallel-sided in male; scutellum highly elevated above postscutellum; T2–T3 longer than width; sides of T4–T7 strongly bending downward ventrally; T7 long, with dorsal profile convex in lateral view ..... ***Limerodops*** Heinrich, 1949
– Metasoma wide, T3–T6 not elongate; scutellum slighly elevated above postscutellum; T7 normal ... ***Diphyus*** Kriechbaumer, 1890

7. Gastrocoeli large and deep; S4 of female separated by median unsclerotized area with longitudinal fold (except *Serratichneumon*) 8
– Gastrocoeli not distinctly deep; S4 of female completely sclerotized 10

8. Propodeum of female without distinct carinae; scutellum slightly elevated above postscutellum; S4 sclerotized; flagellum of male without tyloids, strongly serrate ..... ***Serratichneumon*** Riedel & Sheng, 2023
– Propodeum of female with distinct carinae; scutellum highly elevated above postscutellum; S4 largely unsclerotized; flagellum of male with or without tyloids, not serrate 9

9. Occipital carina joining hypostomal carina above base of mandible; thyridium narrower than interval between them; propodeum with tubercle in area basalis, area superomedia square or narrowed apically; flagellum of male with tyloids; abdominal sternum 9 of male without knoll-shaped swelling ..... ***Hepiopelmus*** Wesmael, 1845
– Occipital carina joining hypostomal carina at base of mandible; thyridium wider than interval between them; propodeum with area basalis lacking tubercle, area superomedia hexagonal; flagellum of male without tyloids; abdominal sternum 9 of male with knoll-shaped swelling ..... ***Tricholabus*** Thomson, 1894

10. Second segment of maxillary palp not enlarged; T1 with postpetiole coriaceous or weakly rugose ..... ***Achaius*** Cameron, 1903
– Second segment of maxillary palp enlarged; T1 with postpetiole smooth and sparsely punctate; T2 minutely or coarsely punctate between gastrocoeli 11

11. Propodeum with area dentipara having carina transforming to broad tooth-like projection apically, area superomedia wider than long, with anterior transverse carina present laterally; mandibles short, with upper tooth longer than flattened, rounded lower tooth; T2 coarsely punctate between gastrocoeli ..... ***Achaiusoides*** Tereshkin, 2011
– Propodeum with area dentipara having small tooth apically, area superomedia longer than wide, with anterior transvers carina absent laterally; mandibles long and evenly narrowed apically, with upper tooth longer than lower tooth; T2 minutely punctate between gastrocoeli ..... ***Montichneumon*** Chen & Kikuchi gen. nov.

Montichneumon immortalibestia Chen & Kikuchi gen. et sp. nov.
urn:lsid:zoobank.org:act:7FD7584D-9E45-4017-B3BE-A23555A8EDB6
Figs 2–6; Table 2

Diagnosis

See genus.

Etymology

The specific name '*immortalibestia*' is derived from the Latin words '*immortali-*' ('immortal') plus '*bestia*' ('beast'), meaning 'the undying beast'. The name refers to the superhero character 'Wolverine' from the Marvel Comics series 'X-Men', who has the abilities of regeneration and beast-like retractable metal claws, as the yellow and black color pattern of this species resembles the costume of this character. Specific name is a noun in apposition.

Type material

Holotype

TAIWAN • ♀; Miaoli County, Tai'an Township, Shei-Pa National Park, Sian campground of Mt Danan (site SBM11); 24°21′40.3″ N, 121°9′48.59″ E; elev. 3090 m; 27 Jun.–25 Aug. 2021; Jung-Chang Chen, Kuang-Yao Chen, Li-Jen Chang, Ta-Hsiang Li and Hung-Yang Shen leg.; Malaise trap; GenBank nos: PQ361201 (COI), PQ361981 (28S); NMNS ENT 8951-22 (SP0026).

Paratypes

TAIWAN • 1 ♀; Miaoli County, Tai'an Township, Shei-Pa National Park, Xishishan forest road 9.0 K; 24°19′1.89″ N, 121°3′36.28″ E; elev. 2630 m; 16 Nov. 2021–21 Apr. 2022; Jung-Chang Chen, Kuang-Yao Chen, Li-Jen Chang, Ta-Hsiang Li and Hung-Yang Shen leg.; Malaise trap; GenBank nos: PQ361202 (COI); NMNS ENT 8951-23 (SP0072) • 1 ♀; Nantou County, Ren'ai Township, Nanhuashan (= Nenggao Shan North Peak); 6 May 1992; Yang and Huang leg.; sweeping; NMNS ENT 1447-2018 • 1 ♂; Taichung City, Heping District, Eastern peak of Mt Syueshan–369 Cabin; elev. 3000–3200 m; 26–27 Aug. 2021; Chi-Ting Hsu leg.; sweeping; GenBank nos: PQ361203 (COI); NCHU SP0079.

Description

Measurements are based on two females and one male.

Female

Head (Fig. 3B–D). Head in dorsal view 1.8–2.0 (2.0)× as wide as long; frons polished and smooth; OD = 0.15–0.17 (0.17) mm; POL/OD = 1.1–1.2 (1.1); OOL/OD = 1.3–1.4 (1.3); ocellar area rugose-punctate; vertex coarsely punctate with short setae anterior to mid ocellus, finely coriaceous without setae lateral to lateral ocelli; temple evenly punctate with long black setae; occipital carina strong and complete, meeting hypostomal carina above mandible base by 0.6 (0.6)× basal mandible width; face 1.8–2.0 (1.8)× as wide as high, polished and strongly punctate with punctures dense laterally (distance between punctures 0.5–1.0× puncture diameter) and sparse medially (distance between punctures 1.4–1.6× puncture diameter), convex in lateral view; clypeus 2.7 (2.7)× as wide as high, polished and sparsely punctate with distance between punctures 2.4–2.8× puncture diameter, weakly and finely coriaceous medially, with ventral margin truncate, weakly convex in lateral view; labrum exposed, rounded ventrally with row of long setae; malar space long, 1.4–1.5 (1.4)× as long as basal mandible width, finely coriaceous with even and strong punctures; gena wide, 0.8–0.9 (0.8)× as wide as maximum width of eye in lateral view, sparsely punctate with sparse setae; mandible bidentate and evenly narrowed to apex (almost parallel-sided), with upper tooth longer than lower tooth; flagellum with 41–42 segments, first flagellomere 3.1–3.7 (3.1)× as long as wide, 1.4 (1.4)× as long as second flagellomere, second flagellomere 2.2–2.8 (2.2)× as long as wide.

Mesosoma (Fig. 3A, E–F). Pronotum evenly and strongly punctate, with rugose striae ventro-anteriorly and transverse groove dorsally; epomia weak; mesoscutum 1.1–1.3 (1.3)× as long as wide, polished and evenly punctate; notaulus indistinct, present on about anterior half; scutellum 0.9–1.0 (1.0)× as long as wide, flat in lateral profile, polished and sparsely punctate (distance between punctures 3.8–5.0× puncture diameter), with lateral carina absent; metanotum polished and sparsely punctate; mesopleuron polished and evenly punctate, with dorsal half sparsely punctate (distance between punctures 3.0–6.0× puncture diameter), dorso-anterior and ventro-posterior corners rugose; episternal scrobe distinct, mesopleural sulcus absent, epicnemial carina complete and distinct, strongly curved ventrally and 0.9× as high as anterior margin of mesopleuron; metapleuron coarsely punctate and rugose in ventro-posterior corner, with juxtacoxal carina present in anterior half, submetapleural carina complete; propodeal spiracle 3.9–4.2 (3.9)× as long as wide; propodeum with area basalis, area superomedia, and area petiolaris rugose, other area rugose-punctate; area superomedia long, about 1.3× as long as its maximum width; area dentipara with short and indistinct tooth posteriorly; lateromedian longitudinal carina and lateral longitudinal carina complete, anterior transverse carina present medially and absent laterally, posterior transverse carina present but indistinct laterally.

Legs (Fig. 2). Legs evenly punctate with setae; fore femur 3.6–3.8 (3.6)× as long as wide; hind femur 4.9–5.4 (5.4)× as long as wide, 0.8 (0.8)× as long as hind tibia; hind first tarsomere 9.1–9.9 (9.1)× as long as wide, 2.0–2.1 (2.0)× as long as second tarsomere.

Wings (Fig. 4A). Fore wing length 10.0–10.6 (10.6) mm, 3.7–3.8 (3.8)× as long as wide; areolet truncate and tapered anteriorly, 2rs-m 0.9–1.0 (1.0)× as long as 3rs-m, anterior margin of areolet 0.4–0.5 (0.4)× as long as 2rs-m; 1/M 1.1–1.2 (1.2)× as long as 2/M; 1cu-a straight and inclivous, distad M&RS by 0.3–0.4 (0.3)× its length. Hind wing with 2–3 basal hamuli and 9–12 distal hamuli; NI = 4.4–4.5 (4.4).

Metasoma (Figs 3F–G, 4C–D). Tergites and sternites polished; T1 2.2–2.5 (2.5)× as long as its maximum width, 2.7–2.9 (2.9)× as long as its posterior width, 0.9 (0.9)× as long as T2; postpetiole smooth, sparsely and minutely punctate laterally; spiracles of T1 located at about 0.7 of length of tergite; T2 1.3–1.4 (1.4)× as long as its posterior width, evenly and minutely punctate; gastrocoelus indistinct, narrow and long, interval between gastrocoeli about 5.6× gastrocoelus width; thyridium indistinct and transverse, narrower than interval between thyridia; T3 1.0 (1.0)× as long as its posterior width; tergites

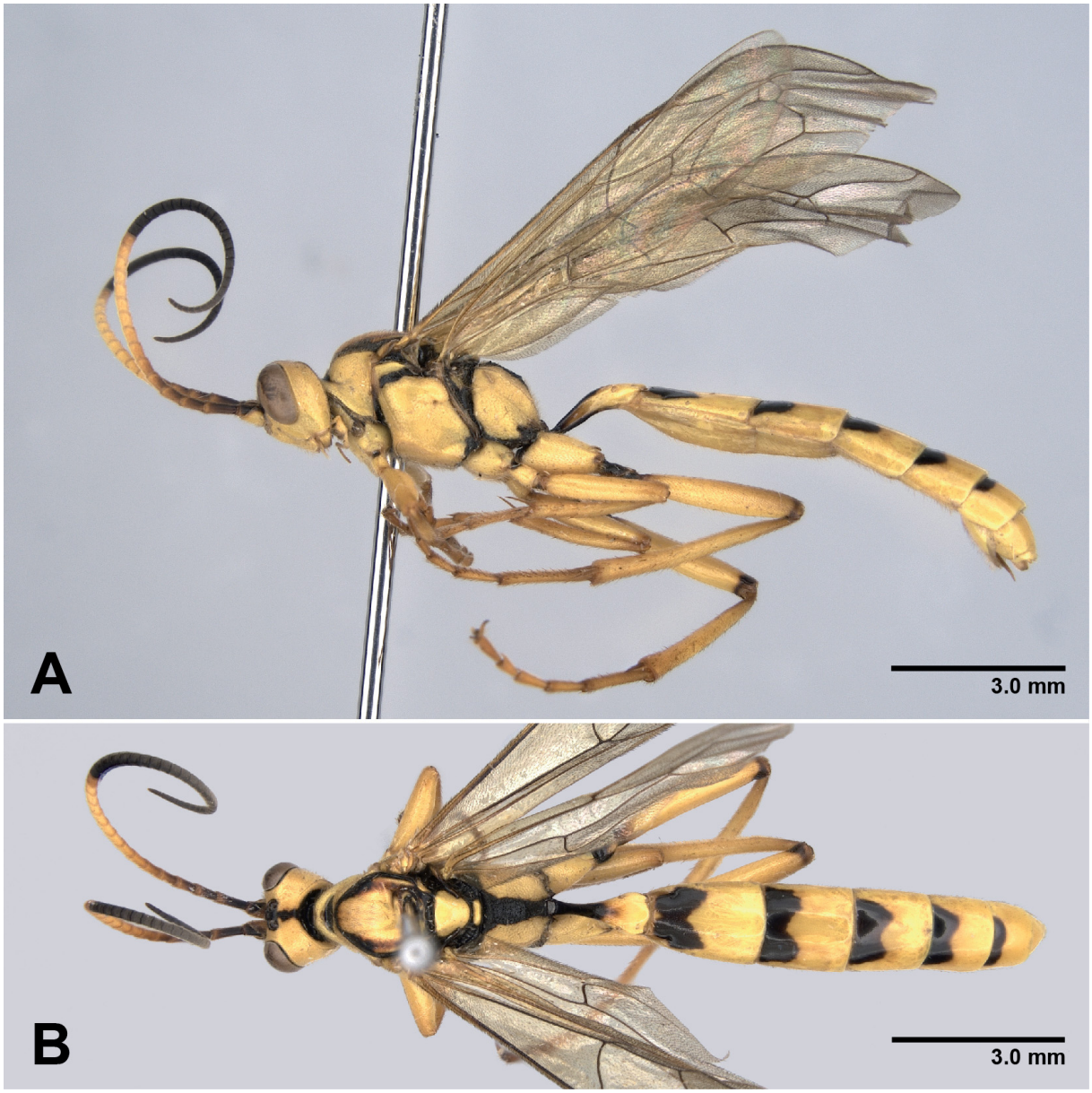

Fig. 2. *Montichneumon immortalibestia* Chen & Kikuchi gen. et sp. nov., holotype. ♀ (NMNS ENT 8951-22). **A**. Habitus in lateral view. **B**. Habitus in dorsal view. Photographed by HPC.

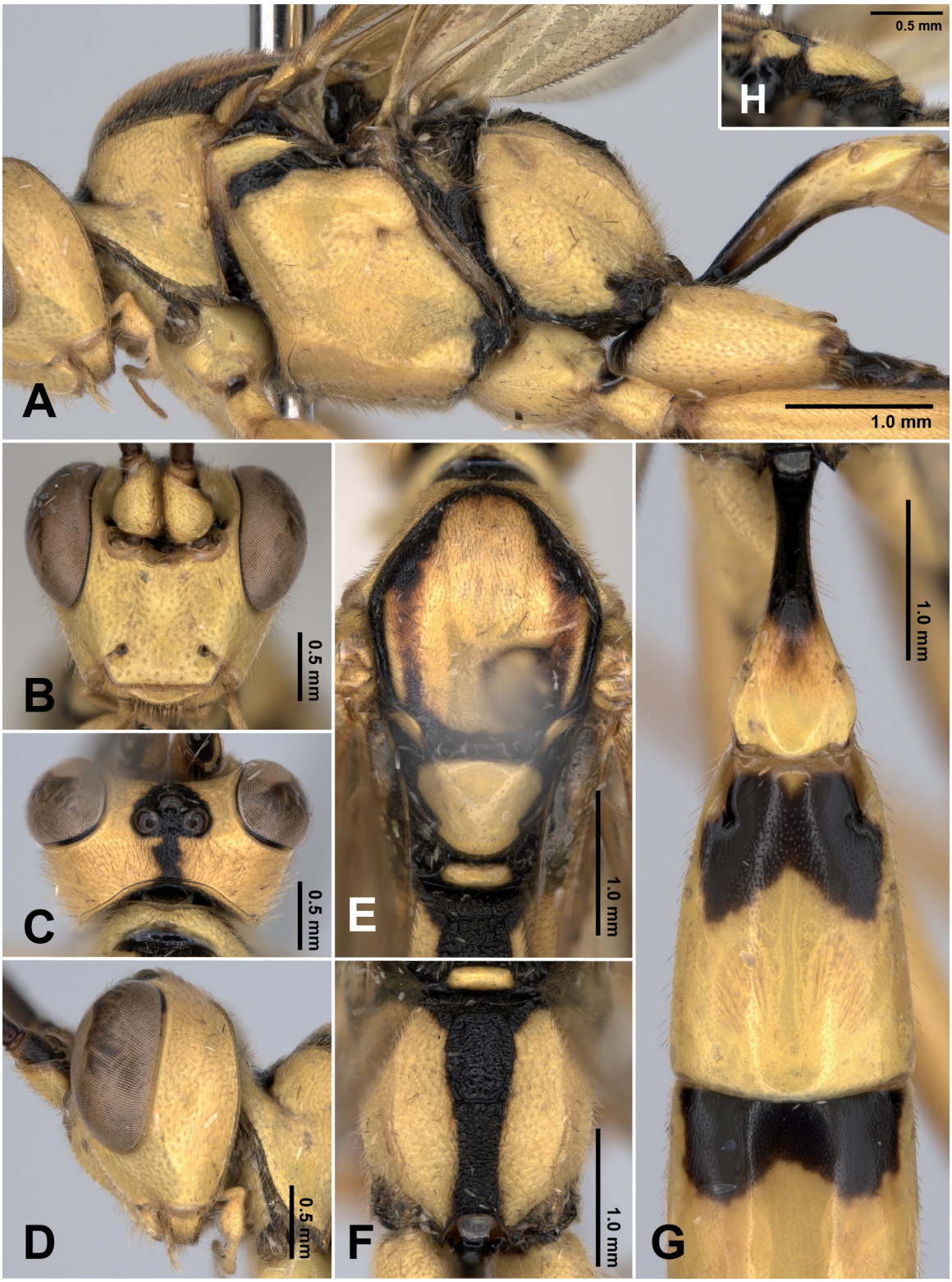

Fig. 3. *Montichneumon immortalibestia* Chen & Kikuchi gen. et sp. nov. **A–G**. Holotype, ♀ (NMNS ENT 8951-22). **H**. Paratype, ♀ (NMNS ENT 8951-23). **A**. Mesosoma in lateral view. **B**. Head in anterior view. **C**. Head in dorsal view. **D**. Head in lateral view. **E**. Mesoscutum and scutellum in dorsal view. **F**. Propodeum in dorsal view. **G**. First to third metasomal tergites. **H**. Scutellum in lateral view. Photographed by HPC.

after T2 evenly (sparsely) and minutely punctate; sternites weakly sclerotized and finely coriaceous; S2 and S3 separated by median unsclerotized area, longitudinally folded, laterosclerites narrow, elongate and tapered anteriorly (S2) and rectangular (S3), S4–S6 completely sclerotized; laterosternites present on S2–S5; S6 (hypopygium) tapered and truncate on posterior margin; metasoma with its apex amblypygous; ovipositor sheath with exposed part 0.8–1.0 (1.0) × as long as wide.

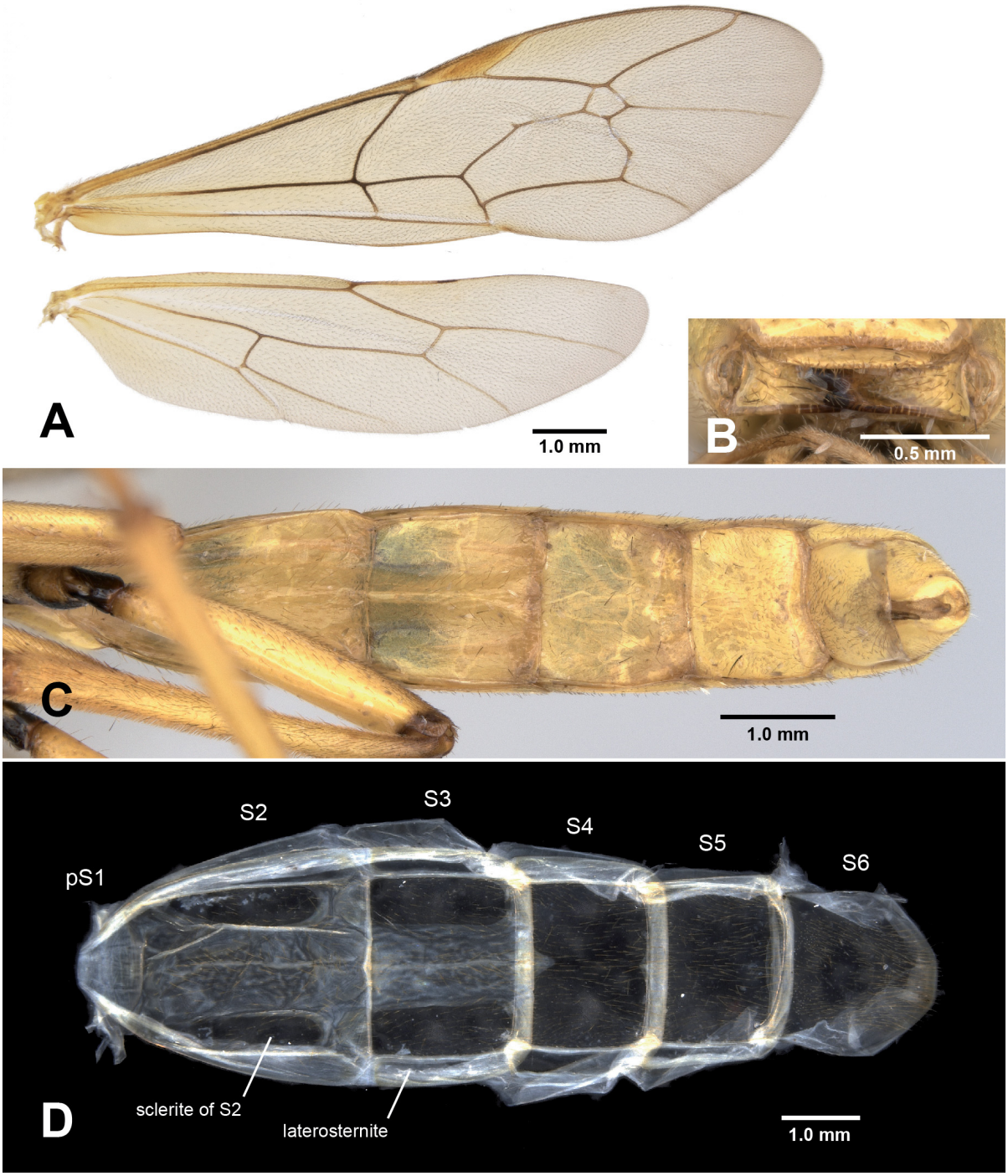

Fig. 4. *Montichneumon immortalibestia* Chen & Kikuchi gen. et sp. nov. **A, D**. Paratype, ♀ (NMNS ENT 8951-23). **B–C**. Holotype, ♀ (NMNS ENT 8951-22). **A**. Wings. **B**. Mandibles. **C**. Metasomal sternites in dried specimen. **D**. Dissected metasomal sternites. Photographed by HPC.

Coloration (Figs 2–4). Head mainly yellow; ocellar area, medial longitudinal line of temple, frons, tentorial pit, mandibular teeth, and occiput black; antenna black, except flagellomeres 1–4 tinged with reddish brown, ventral surface of scape and flagellomeres 5–14 yellow. Mesosoma mainly yellow; dorsal groove of pronotum, margins, antero-lateral corner, and postero-lateral sides of mesoscutum, ventro-lateral margin of scutellum, epicnemium, ventro-posterior corner and transverse line on antero-dorsal corner of mesopleuron, upper division of metapleuron (except one circular marking), anterior and ventral margins of metapleuron, area basalis, area superomedia, and area petiolaris of propodeum black; two linear longitudinal markings on lateral lobes of mesoscutum reddish brown. Wing hyaline tinged with yellowish brown, veins blackish brown, pterostigma yellowish brown. Legs mainly yellow; small markings on fore and mid first trochanters dorsal-basally, basal surface of hind coxa, hind trochanters, basal and apical $^{1}/_{10}$ of hind femur black, tarsi yellow tinged with reddish brown. Metasoma mainly yellow; dorsal and ventral surfaces of T1 petiole and two connected markings in anterior $^{3}/_{10}$ to anterior half of all tergites black; latero-anterior sides of T1 tinged with reddish brown.

Male

General structures similar to female.

Head (Fig. 5A–B). Head in dorsal view 2.0 × as wide as long; OD = 0.15 mm; POL/OD = 1.6; OOL/OD = 1.5; face 1.6 × as wide as long; clypeus 2.8 × as wide as long; malar space 1.1 × as long as basal mandible width; occipital carina meeting hypostomal carina above mandibular base by 0.5 × basal mandible width; gena 0.8 × as wide as maximum width of eye in lateral view; flagellum with 42–43 segments, with tyloids on outer surface of segments 9–19, each segment convex on inner side; first flagellomere 2.9 × as long as wide, 1.4 × as long as second flagellomere; second flagellomere 2.0 × as long as wide.

Mesosoma (Fig. 5C). Mesoscutum 1.3 × as long as wide; scutellum 1.3 × as long as wide; propodeal spiracle 3.5 × as long as wide.

Wings. Fore wing length 10.2 mm, 3.7 × as long as wide; 2rs-m 1.1 × as long as 3rs-m, anterior margin of areolet 0.4 × as long as 2rs-m; 1/M 1.1 × as long as 2/M; 1cu-a distad M&RS by 0.3 × its length. Hind wing with 2–3 basal hamuli and 11–12 distal hamuli; NI = 5.1.

Legs. Fore femur 3.9 × as long as wide; hind femur 6.9 × as long as wide, 0.8 × as long as hind tibia; hind first tarsomere 11.2 × as long as wide, 1.9 × as long as second tarsomere.

Metasoma (Fig. 5D–G). T1 2.5 × as long as its maximum width, 2.9 × as long as its posterior width, 0.9 × as long as T2; T2 1.5 × as long as its posterior width; T3 1.1 × as long as its posterior width. Gonostyle short, tapered, roundly pointed, covered with long setae apically; gonossiculus long and ventrally curved, strongly tapered and pointed in ventro-apical corner, rounded in dorso-apical corner; cuspis large, rounded apically; volsella covered with patch of slender setae; penisvalva with valviceps long, strongly and ventrally curved and narrowed at middle, apex of valviceps rounded in profile, valvura straight and short, about 0.5 × as long as valviceps; abdominal sternum 9 (hypopygium) strongly and triangularly convex on apical margin, without any additional structure.

Coloration (Fig. 5A–D). Similar to female except head in dorsal view with two black markings postero-laterally and one broad longitudinal black stripe medially; mesoscutum with lateral lobes entirely black and medial lobe black anteriorly with one short longitudinal linear black marking; antenna black with flagellomeres 1–13 yellowish-brown ventrally and tyloids reddish brown; metasomal tergites behind T1 with one anterior black marking truncated (T2) or rounded (other tergites behind) on posterior margin.

Distribution

Taiwan.

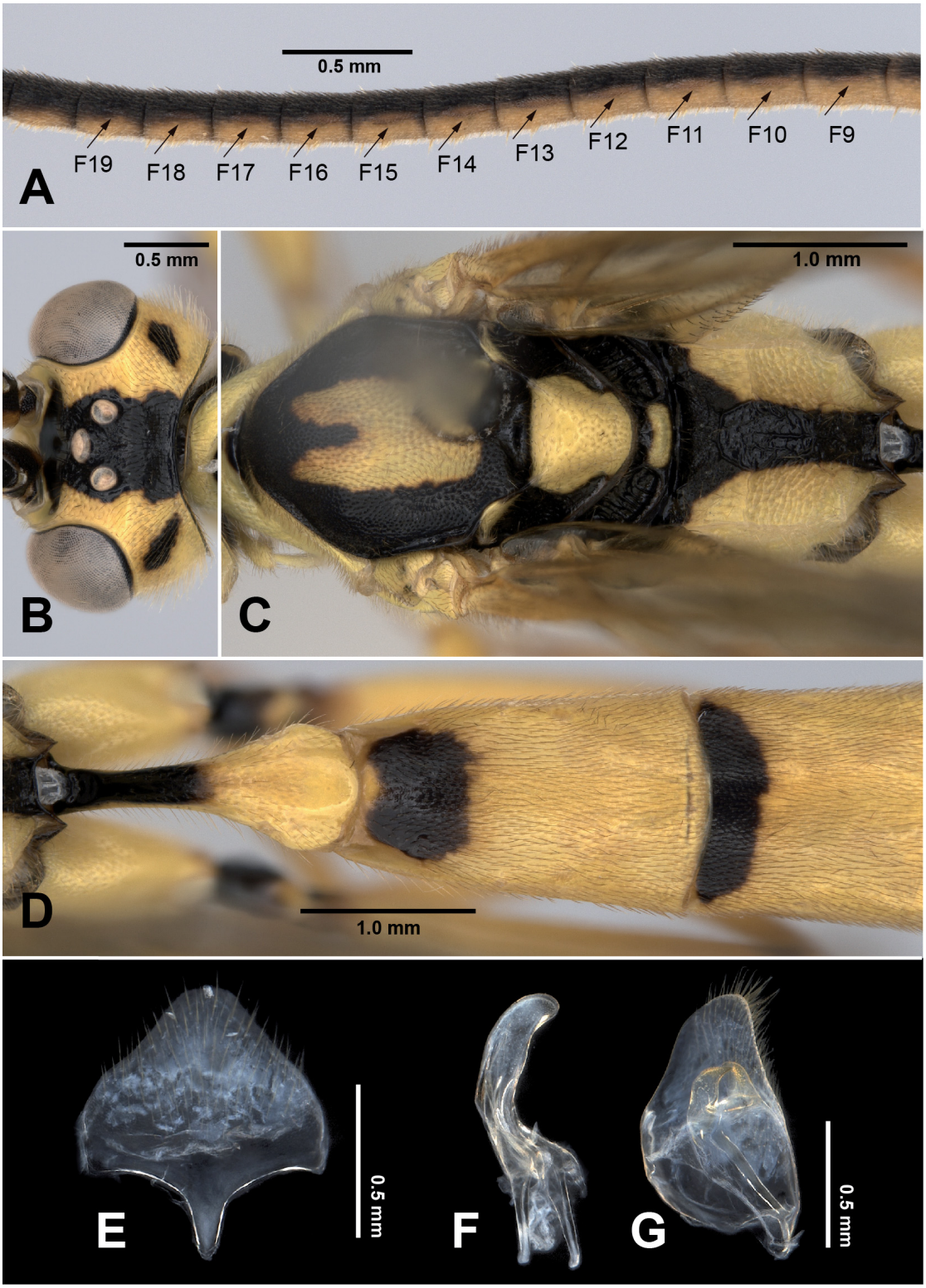

Fig. 5. *Montichneumon immortalibestia* Chen & Kikuchi gen. et sp. nov., paratype, ♂ (NCHU SP0079). **A**. Flagellum, the black arrow indicates the tyloid, and "F plus number" refer to the flagellomere segments. **B**. Head in dorsal view. **C**. Mesosoma in dorsal view. **D**. First to third metasomal tergites. **E**. Abdominal sternum 9. **F**. Penisvalva (dorsal on the left side). **G**. Inner side of right gonostyle (dorsal on the left side). Photographed by HPC.

Bionomics

The host is unknown. This species is distributed in the high-elevation area of central Taiwan (above 2600 m elevation). The holotype was collected in forest margin with *Luzula campestris* (L.) DC. (Juncaceae) grassland (Fig. 6A); one female paratype was collected in pure forest of *Pinus taiwanensis* Hayata, 1911 (Pinaceae) and *Chamaecyparis formosensis* Matsum. (Cupressaceae) (Fig. 6B–C).

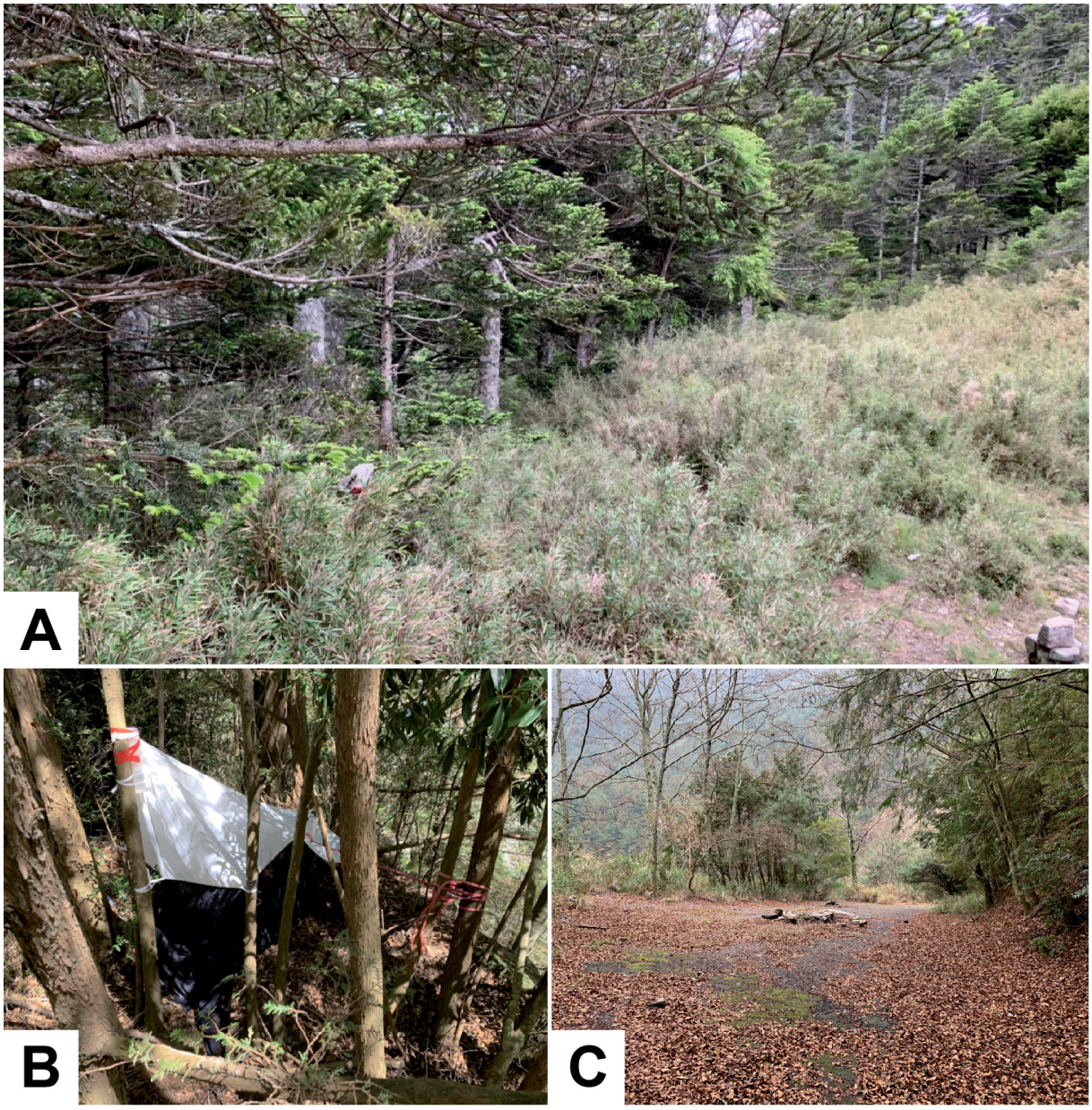

Fig. 6. Habitats of *Montichneumon immortalibestia* Chen & Kikuchi gen. et sp. nov. **A**. Habitat of the holotype, ♀ (NMNS ENT 8951-22) in the Sian campground of Mt Danan (24°21′40.3″ N, 121°9′48.59″ E). **B**. Habitat of the paratype, ♀ (NMNS ENT 8951-23) on Xishishan forest road (24°19′1.89″ N, 121°3′36.28″ E). **C**. Ditto. Photographed by T.-H. Lee (A–B) and Y.-M. Hsu (C).

Remarks

This species keys to the subtribe Amblytelina (Ichneumonini) in the key of Tereshkin (2009) but does not agree with any genus listed in Tereshkin (2011).

The yellow-black color pattern of this new species is similar to that of two species of the genus *Hedyjoppa* Cameron, 1904. including *H. aurantacea* Cameron, 1904 and *H. chinensis* Riedel, 2023. However, these species can be separated by generic characters such as the length of the malar space (long in *M. immortalibestia* but short in *Hedyjoppa*), the sculpture of the T2 (evenly and minutely punctate in *M. immortalibestia* but striate in *Hedyjoppa*), and the presence of the lateral carina of the scutellum (absent in *M. immortalibestia* but complete in *Hedyjoppa*).

Discussion

In the present phylogeny (Fig. 1), *Montichneumon* gen. nov. clustered within a clade that includes several genera of the *Amblyteles* genus-group and genera previously classified as Amblytelina by Heinrich (1967a), including *Spilichneumon*, *Limerodops*, *Diphyus*, *Achaius*, *Eutanyacra*, and *Amblyteles*. These genera (excluding *Spilichneumon* and *Limerodops* but including *Ctenichneumon*) also formed a strongly supported clade in a more comprehensive UCE-based phylogeny, along with other Nearctic, Oriental, and Neotropical genera: *Ectopimorpha* Viereck, 1912, *Oreohoplis* Townes, 1966, *Neodiphyus* Heinrich, 1977, *Netanyacra* Heinrich, 1968, *Setanta* Cameron, 1901, and *Thymebatis* Brèthes, 1909 (Santos *et al.* 2021). It is necessary to include *Montichneumon* in a more comprehensive phylogeny to understand its phylogenetic relationship to other ichneumonine genera.

Despite the morphology of *Montichneumon* gen. nov. being most similar to *Hepiopelmus* (e.g., smooth postpetiole, unsclerotized S2–S3 of females with longitudinal fold, and narrower gastrocoeli), we found that *Hepiopelmus* was not closely related to the *Amblyteles* genus-group (Fig. 1). It suggests that the classification of Heinrich (1967a, 1967b, 1974a, 1977) may not reflect the evolutionary history of this group, as supported by Santos *et al.* (2021).

Amblypygy is a convergent trait that evolved multiple times within the subfamily Ichneumoninae, corresponding with attacking larval hosts (Santos *et al.* 2021). Therefore, although the host is unknown for *Montichneumon* gen. nov., its amblypygous female metasomal apex suggests it may oviposit into larval lepidopterans.

The color pattern of *Montichnumon* gen. nov., a yellow background with black longitudinal stripes on the mesoscutum, ocellar area, propodeum, and transverse black stripes on the metasomal tergites, is also notable as it resembles that of other Oriental ichneumonines found at high elevations. It has been observed in, for example, *Hedyjoppa chinensis* Riedel, 2023, *Hepiopelmus gongshanus* Riedel, 2023 (Riedel 2023), *Diphyus charlottae* (Heinrich, 1965), *D, malaisei* (Heinrich, 1965), *D. victoriae* (Heinrich, 1965) (Heinrich 1965a), *Hepiopelmus flavomaculatus* (Cameron, 1903) (Cameron 1903), and *Hedyjoppa aurantacea* Cameron, 1904 (Cameron 1904), all found in high-elevation areas of the Oriental region. Additional Taiwanese specimens identified as undescribed *Hepiopelmus* and *Hedyjoppa* species, discovered by the first author, also exhibit this color pattern and were collected at high altitudes (Supp. file 3). These findings suggest a potential association between this color pattern and high elevation distribution in the Oriental region. A more comprehensive investigation of the Oriental fauna is necessary to explore the distributional pattern of this trait further.

Acknowledgments

We would like to express our sincere thanks to Yu-Feng Hsu, Yu-Ming Hsu, and Kuang-Yao Chen (Department of Life Science, National Taiwan Normal University, Taipei, Taiwan), and Jung-Chang

Chen, Li-Jen Chang, Ta-Hsiang Li, and Hung-Yang Shen for the specimens collecting under their project SP110113 ("A survey for selection of insect indicator species and their microhabitat usage in the Daxueshan area of Shei-Pa National Park"); Wen-Bin Yeh and Chi-Ting Hsu (Department of Entomology, National Chung Hsing University) for the specimens collecting under the permission 1100001636 from Shei-Pa National Park; Matthias Riedel (Zoologische Staatssammlung München, Germany) for providing literature and suggestions on the generic placement of the new species; Sheng-Shan Lu, Wen-Chi Yeh, Ling-Mu Jaung, and Yun-Yin Yeh (TFRI) for their kind supports during the specimen investigation of the first author. We also thank two anonymous reviewers and the subject editor, Gavin Broad, for their valuable comments and editorial suggestions, which greatly improved the quality of our manuscript. This study was funded by Taiwan's National Science and Technology Council [grant to the corresponding author: 111-2621-B-002-002] and Animal and Plant Health Inspection Agency, Ministry of Agriculture [grants to the corresponding author: 111AS-5.3.3-BQ-B2(2), 112AS-5.3.3-BQ-B2(2), and 112-RA-BQ-01(Z)].

References

Broad G.R., Shaw M.R. & Fitton M.G. 2018. Ichneumonid Wasps (Hymenoptera: Ichneumonidae): their classification and biology. *Handbooks for the Identification of the British Insects* 7 (12): 1–418. https://doi.org/10.1079/9781800625471.0000

Cameron P. 1903. Descriptions of twelve new genera and species of Ichneumonidae (Heresiarchini and Amblypygi) and three species of *Ampulex* from the Khasia Hills, India. *Transactions of the Entomological Society of London* 51: 219–238. https://doi.org/10.1111/j.1365-2311.1903.tb01136.x

Cameron P. 1904. Descriptions of new genera and species of Ichneumonidae from India. (Hym.). *Zeitschrift für systematische Hymenopterologie und Dipterologie* 4: 217–224.

Chen H.-P., Lin K.-T. & Wu S. 2023. Re-evaluation of the taxonomic confusion of the metallic-blue *Pimpla* Fabricius, 1804 (Hymenoptera: Ichneumonidae: Pimplinae) species in the Oriental region. *Zootaxa* 5357 (2): 270–284. https://doi.org/10.11646/zootaxa.5357.2.5

Chen H.-P., Kikuchi N. & Shiao S.-F. 2024. Discovery of a new *Pseudalomya* Telenga, 1930 (Hymenoptera, Ichneumonidae, Ichneumoninae) species from Taiwan and its implications for the systematic position of this genus. *Journal of Hymenoptera Research* 97: 277–296. https://doi.org/10.3897/jhr.97.119470

Claridge B.R., Kaunisto K.M. & Sääksjärvi I.E. 2023. *Capitojoppa*, a new genus of Ichneumoninae (Hymenoptera, Ichneumonidae) from Peruvian Amazonia. *ZooKeys* 1178: 69–76. https://doi.org/10.3897/zookeys.1178.108929

Dal Pos D., Claridge B., Diller E., van Noort S. & Di Giovanni F. 2023a. Still counting: new records, nomenclatural notes, and three new species of Phaeogenini (Hymenoptera, Ichneumonidae, Ichneumoninae) from the Afrotropical region. *European Journal of Taxonomy* 868 (1): 1–71. https://doi.org/10.5852/ejt.2023.868.2105

Dal Pos D., Mikó I., Talamas E.J., Vilhelmsen L. & Sharanowski B.J. 2023b. A revised terminology for male genitalia in Hymenoptera (Insecta), with a special emphasis on Ichneumonoidea. *PeerJ* 11: e15874. https://doi.org/10.7717/peerj.15874

Eady R.D. 1968. Some illustrations of microsculpture in the Hymenoptera. *Proceedings of the Royal Entomological Society of London* 43: 66–72. https://doi.org/10.1111/j.1365-3032.1968.tb01029.x

Folmer O., Black M., Hoeh W., Lutz R. & Vrijenhoek R. 1994. DNA primers for amplification of mitochondrial cytochrome c oxidase subunit I from diverse metazoan invertebrates. *Molecular Marine Biology and Biotechnology* 3 (5): 294–299.

Gauld I.D. 1991. *The Ichneumonidae of Costa Rica, 1*. Memoirs of the American Entomological Institute 47: 1–589.

Guindon S., Dufayard J.-F., Lefort V., Anisimova M., Hordijk W. & Gascuel O. 2010. New algorithms and methods to estimate maximum-likelihood phylogenies: Assessing the performance of PhyML 3.0. *Systematic Biology* 59 (3): 307–321. https://doi.org/10.1093/sysbio/syq010

Gupta S. 1988. New distributional records for Ichneumoninae (Hymenoptera: Ichneumonidae) of the Indo-Australian area. *Oriental Insects* 22 (1): 301–357.

Heinrich G.H. 1965a. Burmesische Ichneumoninae I. *Entomologisk Tidskrift* 86: 74–130.

Heinrich G.H. 1965b. Burmesische Ichneumoninae II. *Entomologisk Tidskrift* 86: 133–177.

Heinrich G.H. 1966. Burmesische Ichneumoninae III [a]. *Entomologisk Tidskrift* 87: 184–247.

Heinrich G.H. 1967a. *Synopsis and Reclassification of the Ichneumoninae Stenopneusticae of Africa south of the Sahara (Hymenoptera) vol. 1. Introduction; Key to tribes and subtribes of Ichneumoninae Stenopneusticae; Synopsys of the Protichneumonini, Ceratojoppini, Ischnojoppini, Trogini*. Farmington State College Press, Altötting.

Heinrich G.H. 1967b. *Stenopneusticae of Africa south of Sahara (Hymenoptera) vol. III. Synopsis of the Ichneumonini: Subtribes Ichneumonina and Amblytelina*. Farmington State College Press, Altötting.

Heinrich G.H. 1967c. Burmesische Ichneumoninae III [b]. *Entomologisk Tidskrift* 88: 1–32.

Heinrich G.H. 1968a. Burmesische Ichneumoninae IV. *Entomologisk Tidskrift* 89: 77–106.

Heinrich G.H. 1968b. Burmesische Ichneumoninae V. *Entomologisk Tidskrift* 89: 197–228.

Heinrich G.H. 1969. Burmesische Ichneumoninae VI. *Entomologisk Tidskrift* 90: 100–130.

Heinrich G.H. 1970. Burmesische Ichneumoninae VII. *Entomologisk Tidskrift* 91: 68–102.

Heinrich G.H. 1974a. Burmesische Ichneumoninae VIII. *Annales Zoologici* 31 (5): 407–456.

Heinrich G.H. 1974b. Burmesische Ichneumoninae IX. *Annales Zoologici* 32 (8): 103–197.

Heinrich G.H. 1975. Burmesische Ichneumoninae X. *Annales Zoologici* 32 (20): 441–514.

Heinrich G.H. 1977. Ichneumoninae of Florida and neighboring states (Hymenoptera: Ichneumonidae, subfamily Ichneumoninae). *Arthropods of Florida and Neighboring Land Areas* Vol. 9. Florida Department of Agriculture and Consumer Services, Gainesville.

Heinrich G.H. 1980. Burmesische Ichneumoninae XI. *Annales Zoologici* 35 (11): 115–192.

Kalyaanamoorthy S., Minh B.Q., Wong T.K.F., von Haeseler A. & Jermiin L.S. 2017. Modelfinder: Fast model selection for accurate phylogenetic estimates. *Nature Methods* 14: 587–589. https://doi.org/10.1038/nmeth.4285

Kikuchi N. & Konishi K. 2021. A taxonomic revision of the genus *Linycus* Cameron, 1903 from Japan. *Zootaxa* 4948 (4): 546–558. https://doi.org/10.11646/zootaxa.4948.4.3

Laurenne N.M., Broad G. & Quicke D.L.J. 2006. Direct optimization and multiple alignment of 28S D2–D3 rDNA sequences: problems with indels on the way to a molecular phylogeny of the cryptine ichneumon wasps (Insecta: Hymenoptera). *Cladistics* 22: 442–473. https://doi.org/10.1111/j.1096-0031.2006.00112.x188–1195

Minh B.Q., Nguyen M.A.T. & von Haeseler A. 2013. Ultrafast approximation for phylogenetic bootstrap. *Molecular Biology and Evolution* 305: 1188–1195. https://doi.org/10.1093/molbev/mst024

Nguyen L.T., Schmidt H.A., von Haeseler A. & Minh B.Q. 2015. IQ-TREE: a fast and effective stochastic algorithm for estimating maximum-likelihood phylogenies. *Molecular Biology and Evolution* 32 (1): 268–274. https://doi.org/10.1093/molbev/msu300

Ratnasingham S. & Hebert P.D. 2007. BOLD: The Barcode of Life Data System (http://www.barcodinglife.org). *Molecular Ecology Notes* 7 (3): 355–364. https://doi.org/10.1111/j.1471-8286.2007.01678.x

Riedel M. 2019. Contribution to the Ichneumoninae (Hymenoptera, Ichneumonidae) of Nepal. *Linzer Biologische Beiträge* 51: 1119–1162. *Contributions to Entomology* 73 (2): 223–248. https://doi.org/10.3897/contrib.entomol.73.e107542

Riedel M. 2023. Notes on Ichneumoninae (Hymenoptera, Ichneumonidae) from southern China, with descriptions of one new genus and twelve new species. *Contributions to Entomology* 73 (2): 223–248. https://doi.org/10.3897/contrib.entomol.73.e107542

Santos B.F., Wahl D.B., Rousse P., Bennett A.M.R., Kula R. & Brady S.G. 2021. Phylogenomics of Ichneumoninae (Hymenoptera, Ichneumonidae) reveals pervasive morphological convergence and the shortcomings of previous classifications. *Systematic Entomology* 46: 704–724. https://doi.org/10.1111/syen.12484

Sheng M.-L., Riedel M. & Wang Z. 2023. A new genus and species of Ichneumonini Latreille (Hymenoptera, Ichneumonidae, Ichneumoninae) from Oriental Region. *European Journal of Taxonomy* 910 (1): 14–24. https://doi.org/10.5852/ejt.2023.910.2355

Tereshkin A.M. 2009. Illustrated key to the tribes of subfamilia Ichneumoninae and genera of the tribe Platylabini of world fauna (Hymenoptera, Ichneumonidae). *Linzer biologische Beiträge* 41 (2): 1317–1608.

Tereshkin A.M. 2011. Illustrated key to the genera of the subtribe Amblytelina of Palaearctic (Hymenoptera, Ichneumonidae, Ichneumoninae, Ichneumonini). *Linzer biologische Beiträge* 43 (1): 597–711.

Townes H., Townes M. & Gupta V.K. 1961. A catalogue and reclassification of the Indo-Australian Ichneumonidae. *Memoirs of the American Entomological Institute* 1: 1–522.

Trifinopoulos J., Nguyen L.T., von Haeseler A. & Minh B.Q. 2016. W-IQ-TREE: a fast online phylogenetic tool for maximum likelihood analysis. *Nucleic Acids Research* 44 (W1): W232–W235. https://doi.org/10.1093/nar/gkw256

Veijalainen A., Sääksjärvi I.E., Erwin T.L., Gómez I.C. & Longino J.T. 2013. Subfamily composition of Ichneumonidae (Hymenoptera) from western Amazonia: Insights into diversity of tropical parasitoid wasps. *Insect Conservation and Diversity* 6 (1): 28–37. https://doi.org/10.1111/j.1752-4598.2012.00185.x

Yu D.S., van Achterberg C. & Horstmann K. 2016. Taxapad 2016, Ichneumonoidea 2015. Database on flash-drive. Taxapad, Ottawa, Ontario.

Printed versions of all papers are deposited in the libraries of four of the institutes that are members of the *EJT* consortium: Muséum national d'Histoire naturelle, Paris, France; Meise Botanic Garden, Belgium; Royal Museum for Central Africa, Tervuren, Belgium; Royal Belgian Institute of Natural Sciences, Brussels, Belgium. The other members of the consortium are: Natural History Museum of Denmark, Copenhagen, Denmark; Naturalis Biodiversity Center, Leiden, the Netherlands; Museo Nacional de Ciencias Naturales-CSIC, Madrid, Spain; Leibniz Institute for the Analysis of Biodiversity Change, Bonn – Hamburg, Germany; National Museum of the Czech Republic, Prague, Czech Republic; The Steinhardt Museum of Natural History, Tel Aviv, Israël.

Supplementary files

Supp. file 1. Sequences used in this study. Table in the .xlsx file. The cells in blue with bold font indicate the newly obtained sequences in this study. https://doi.org/10.5852/ejt.2025.1007.2997.13465

Supp. file 2. Fasta and Nexus files for the analysis in this study. Files were compressed in the .zip file. Fasta files containing alignments of all markers analyzed in this study, along with the Nexus file specifically for the optimal partition scheme identified based on the concatenated 28S+COI dataset for the analysis. https://doi.org/10.5852/ejt.2025.1007.2997.13467

Supp. file 3. Figure of other specimens for comparison. Two undescribed species of *Hepiopelmus* Wesmeal, 1845 and *Hedyjoppa* Cameron, 1904 that exhibited yellow-black coloration were collected from high-elevation Taiwan. **A**. TFRI72303, *Hepiopelmus* sp., habitus in dorsal view. **B**. TFRI72304, *Hedyjoppa* sp., habitus in dorsal view. https://doi.org/10.5852/ejt.2025.1007.2997.13469